

## Fabrication of One-dimensional SnO<sub>2</sub>/MoO<sub>3</sub>/C Nanostructure Assembled of Stacking SnO<sub>2</sub> Nanosheets from Its Heterostructure Precursor and Its Application in Lithium-Ion Batteries

Lulu Si,<sup>a</sup> Zhengqiu Yuan,<sup>a</sup> Jianwen Liang,<sup>a</sup> Lei Hu,<sup>a</sup> Yongchun Zhu,<sup>\*b</sup> and Yitai Qian<sup>\*a, b, c</sup>

<sup>a</sup> Department of Chemistry, University of Science and Technology of China, Hefei, Anhui 230026, PR China. Fax: (+) 86-551-63601589; E-mail: ytqian@ustc.edu.cn

<sup>b</sup> Hefei National Laboratory for Physical Science at Microscale, University of Science and Technology of China, Hefei, Anhui 230026, PR Chin. Fax: (+) 86-551-63601589; E-mail: ychzhu@ustc.edu.cn

<sup>c</sup> School of Chemistry and Chemical Engineering, Shandong University, Jinan 250100, PR China

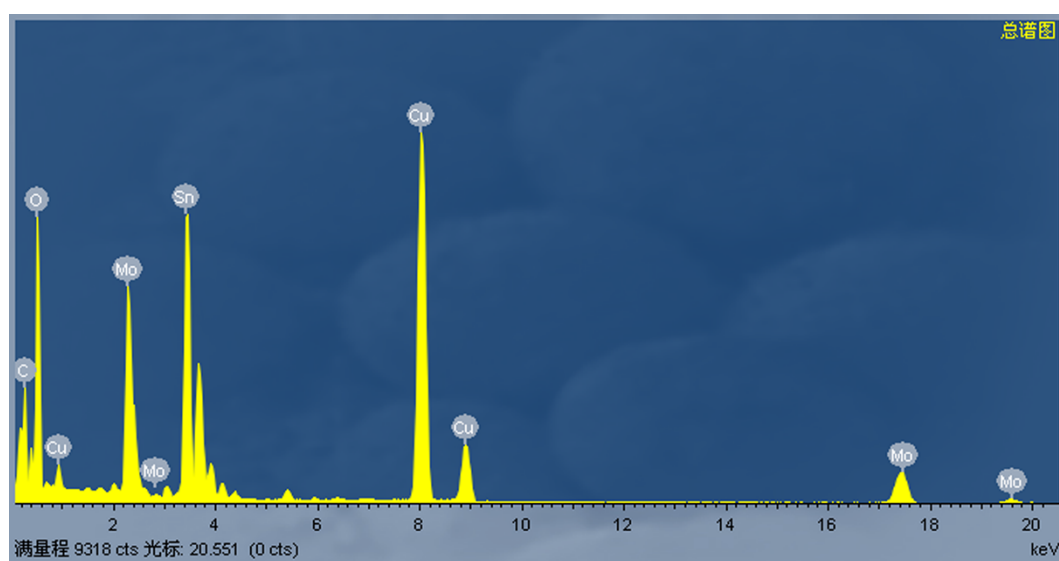


Figure S1. EDS spectrum attached to the SnO<sub>2</sub>/MoO<sub>3</sub>/C nanocomposites

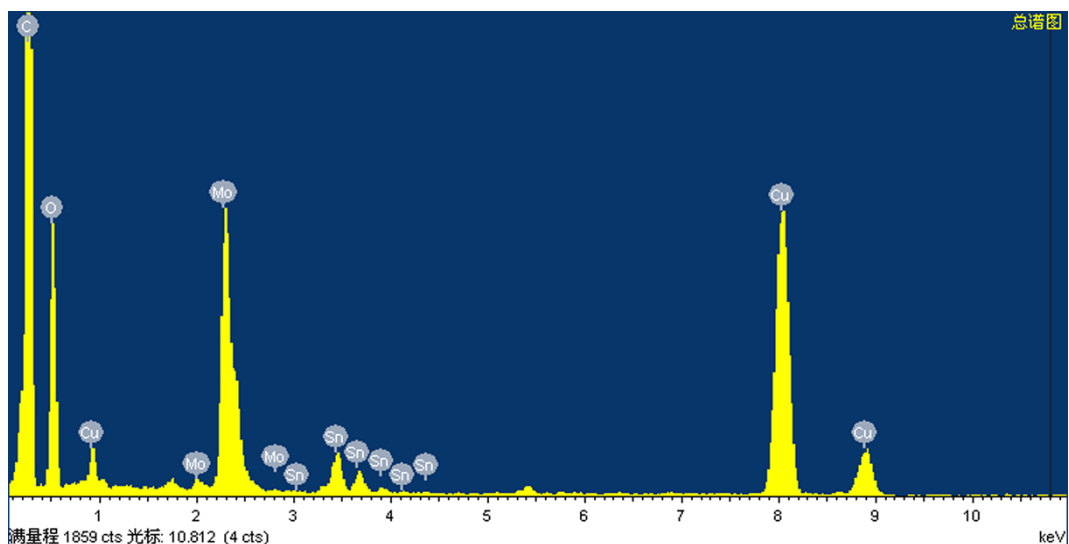


Figure S2. EDS spectrums attached to the TEM of  $S_{6h}$

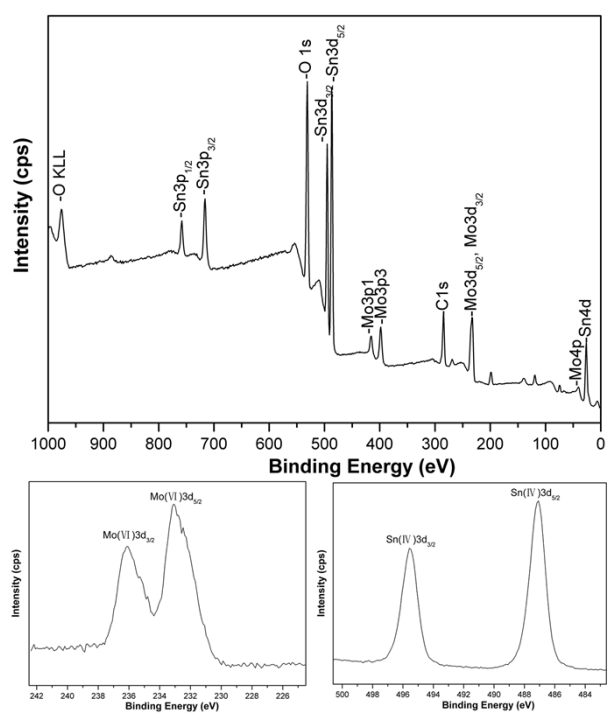


Figure S3. (a) Full-range XPS spectrum of the  $SnO_2/MoO_3$  nanocomposites before carbon coating; (b) the Mo(VI) 3d spectrum and (c) Sn(IV) 3d spectrum.

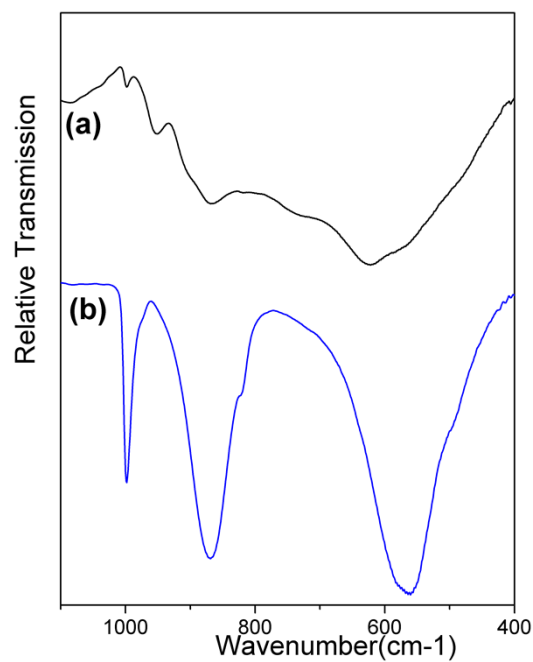


Figure S4. FTIR spectra of (a) the  $\text{SnO}_2/\text{MoO}_3$  nanocomposites before carbon coating, (b) pure crystalline  $\alpha$ - $\text{MoO}_3$

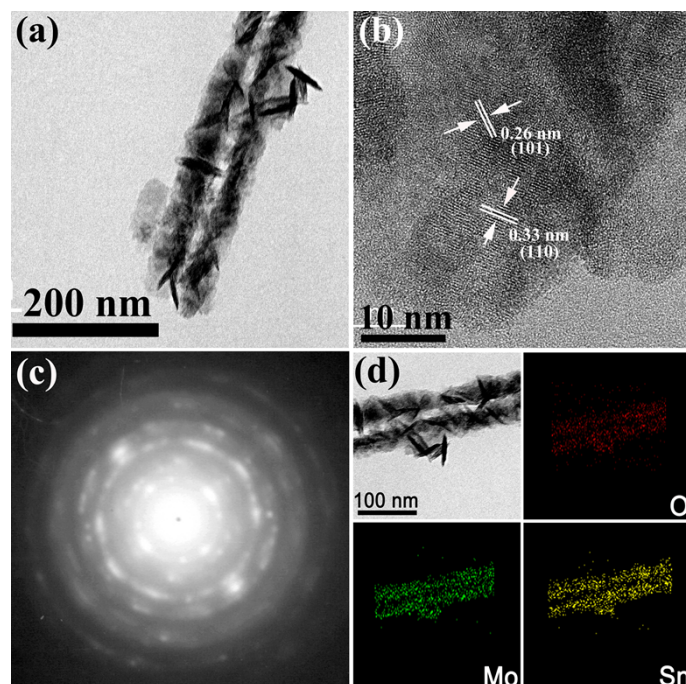


Figure S5. (a) Lower-magnification TEM image of the 1-D  $\text{SnO}_2/\text{MoO}_3$  nanocomposites before carbon coating; (b) HRTEM image of the circular area in (a); (c) Corresponding SAED pattern; (d) corresponding EDS mapping images of O (red), Mo (green), Sn (yellow) and C (purple), respectively

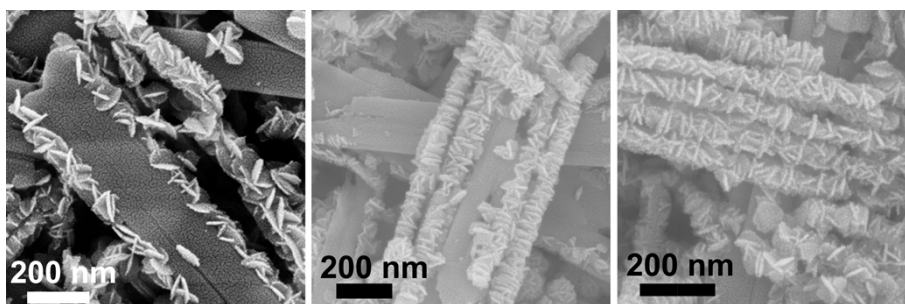


Figure S6. Typical SEM images of the obtained products at various reaction stages by setting the reaction time at the temperature of 150 °C

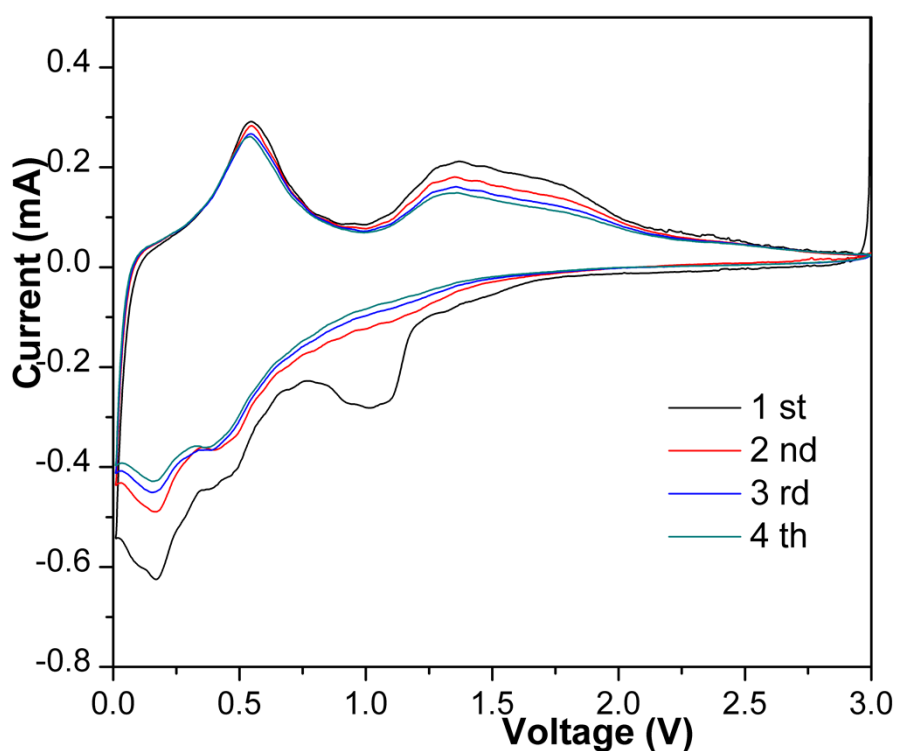


Figure S7. The first four cyclic voltammogram (CV) curves of SnO<sub>2</sub>/MoO<sub>3</sub>/C nanocomposite electrode in the potential range of 0.001-3.0 V at a slow scan rate of 0.2 mV s<sup>-1</sup>.

Figure S7 is the first four cyclic voltammogram (CV) curves of SnO<sub>2</sub>/MoO<sub>3</sub>/C nanocomposite electrode in the potential range of 0.001-3.0 V at a slow scan rate of 0.2 mV s<sup>-1</sup>. The shape of the CV curves of SnO<sub>2</sub>-MoO<sub>3</sub> is similar to the main part nanocrystalline SnO<sub>2</sub>. It is generally accepted that the electrochemical process of SnO<sub>2</sub> anodes can be described by the two principal reactions: (1) SnO<sub>2</sub> + 4Li<sup>+</sup> + 4e<sup>-</sup> → Sn +

$2\text{Li}_2\text{O}$ ; (2)  $\text{Sn} + x\text{Li}^+ + xe^- \leftrightarrow \text{Li}_x\text{Sn}$  ( $0 \leq x \leq 4.4$ ). In the first sweep, the broad cathodic peak around 1.0 V could derive from  $\text{Li}_2\text{O}$  formation and electrolyte decomposition when  $\text{SnO}_2$  nanosheets react with  $\text{Li}^+$  as described in Equation (1). The formation of a solid electrolyte interface (SEI) layer may be another factor. From the second cycle the peak disappeared since the process of  $\text{SnO}_2$  to Sn is generally believed to be irreversible. However, this cathodic peak, together with the anodic peak at 1.3 V, is still present in subsequent cycles, indicating partially reversibility of the reaction. The characteristic pair of current peaks is observed at potentials (cathodic/anodic) of 0.15/0.58 V in the four cycles. This is attributed to the alloying (cathodic sweep) and dealloying (anodic sweep) processes between Li and Sn, the Equation (2), which are observed to be highly reversible and mainly responsible for the reversible lithium storage capacity in Sn-based electrode materials. Different from the typical CV curves of  $\text{SnO}_2$ , the cathodic peak at about 0.40 V exists, which could be attributed to the reduction of  $\text{Li}_x\text{MoO}_3$  to metal Mo and described by the reaction  $\text{Li}_x\text{MoO}_3 + (6-x)\text{Li}^+ + (6-x)e^- \leftrightarrow \text{Mo} + 3\text{Li}_2\text{O}$ . The anodic peak centered at 1.5 V can be assigned to the extraction process of lithium.

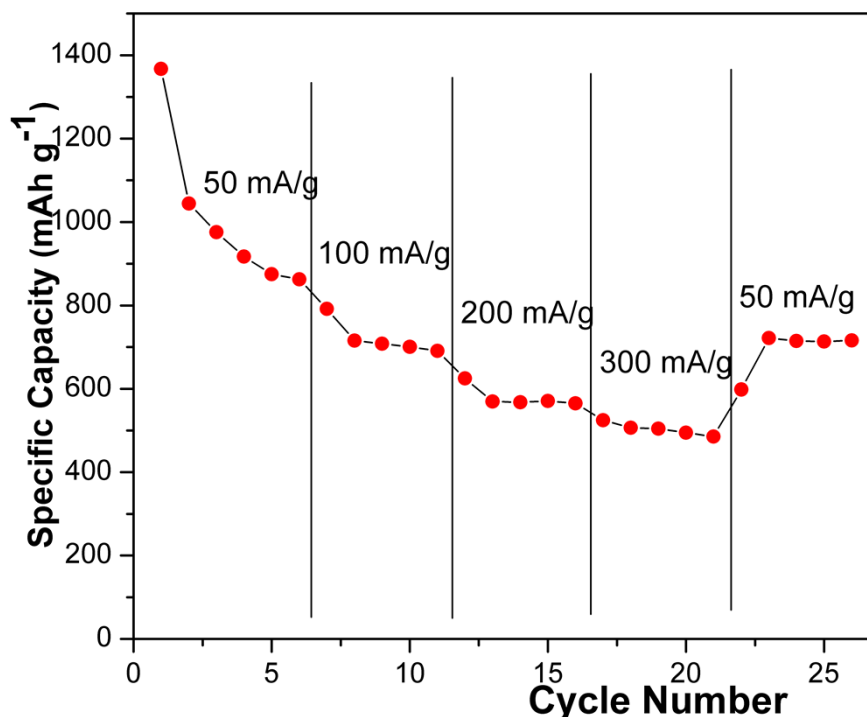


Figure S8. Specific capacities of the  $\text{SnO}_2/\text{MoO}_3/\text{C}$  nanocomposite electrode for different

discharge/charge cycles at various current densities.

The cell with the SnO<sub>2</sub>/MoO<sub>3</sub>/C nanocomposite electrode was evaluated for rate capability and the results are shown in Figure S8. When the current rate was first increased from 50 to 100 mA g<sup>-1</sup>, a stable capacity of around 780 mAh g<sup>-1</sup> could be achieved. Afterwards, the rate was increased stepwise up to 300 mA g<sup>-1</sup>, the electrode could still deliver a stable capacity of about 500 mAh g<sup>-1</sup>. Upon decreasing the current rate to 50 mA g<sup>-1</sup>, a capacity of around 720 mAh g<sup>-1</sup> can be recovered.

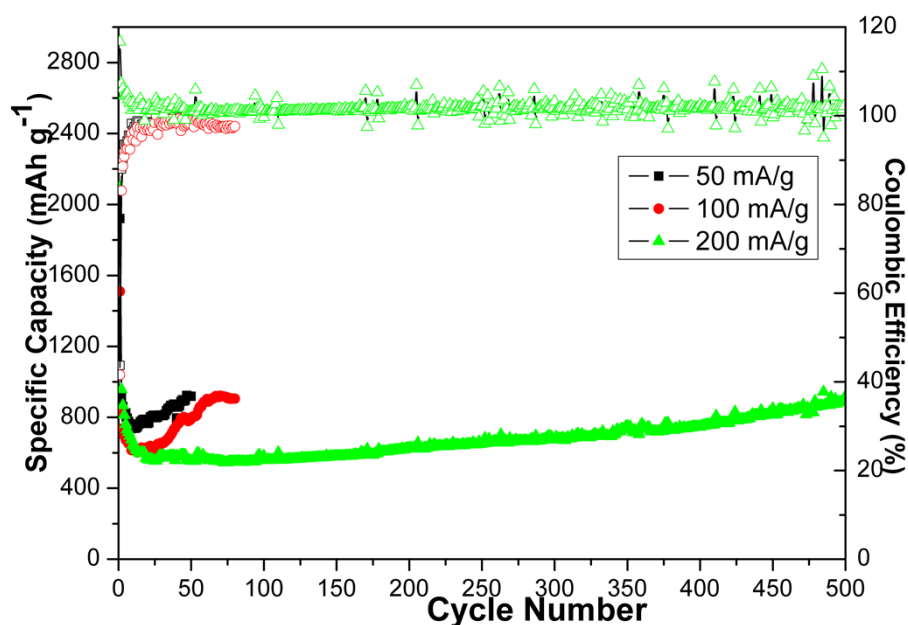


Figure S9. Cycling performance and coulombic efficiency of SnO<sub>2</sub>/MoO<sub>3</sub>/C nanocomposites at different current rates within a voltage window of 0.01–3.0 V.